Electric Power Systems Research 136 (2016) 383–397

Contents lists available at ScienceDirect

Electric Power Systems Research

journal homepage: www.elsevier.com/locate/epsr

Simulated annealing to handle energy and ancillary services joint management considering electric vehicles

Tiago Sousa[a,*], Tiago Soares[b], Hugo Morais[b], Rui Castro[c], Zita Vale[a]

[a] GECAD – Knowledge Engineering and Decision Support Research Center – Polytechnic of Porto (IPP), R. Dr. António Bernardino de Almeida, 431, 4200-072 Porto, Portugal
[b] AUTomation and Control Group – Department of Electrical Engineering, Denmark Technical University (DTU), Elektrovej, Bld 326, 2800 Lyngby, Denmark
[c] INESC-ID/IST Instituto Superior Técnico – University of Lisbon, Lisbon, Portugal

ARTICLE INFO

Article history:
Received 10 July 2015
Received in revised form 16 February 2016
Accepted 16 March 2016
Available online 4 April 2016

Keywords:
Ancillary services
Electric vehicle
Optimal resource scheduling
Simulated annealing
Virtual power player

ABSTRACT

The massive use of distributed generation and electric vehicles will lead to a more complex management of the power system, requiring new approaches to be used in the optimal resource scheduling field. Electric vehicles with vehicle-to-grid capability can be useful for the aggregator players in the mitigation of renewable sources intermittency and in the ancillary services procurement. In this paper, an energy and ancillary services joint management model is proposed. A simulated annealing approach is used to solve the joint management for the following day, considering the minimization of the aggregator total operation costs. The case study considers a distribution network with 33-bus, 66 distributed generation and 2000 electric vehicles. The proposed simulated annealing is matched with a deterministic approach allowing an effective and efficient comparison. The simulated annealing presents a solution closer to the one obtained in the deterministic approach (1.03% error), yet representing 0.06% of the deterministic approach CPU time performance.

1. Introduction

1.1. Motivation and background

Power systems have been changing to cope with the new challenges and ambitious goals on climate and energy policies in the scope of the transition towards a low-carbon economy [1]. For instance, European Union commission committed the member countries for 2020 [2] "*reduction in greenhouse gas emissions to 20% below 1990 levels, 20% share of renewable in the final energy consumption and reduction in primary energy use of 20% below the baseline projection for 2020*". Moreover, in [3] is pointed that power system and transport sectors are the major responsible for the CO_2 emissions. Therefore, electric vehicles (EVs) and distributed generation (DG) based on renewable sources can help on reducing carbon emissions in power system, and also in transport sectors [4]. In fact, renewable sources, namely wind and solar power, have been widely adopted in power system in the last years [5]. More recently, EVs have been proposed to gradually replace the internal combustion engine vehicles in the road transport [6].

In future power systems, the massive use of EVs and DG will represent a significant impact and benefit in the power system, namely at the distribution level, however, its planning and operation will become more complex due to this large DERs penetration. Therefore, smart grid concept can deal with power system planning and operation under this new paradigm, ensuring more efficient, sustainable and safe electricity supply to the consumers as well as integrating large DERs penetration [7]. Gouveia et al. [8] present an overview about the major implementations of smart grid projects in Portugal. About 27% of these smart grid projects are related with the installation of smart meters. In [9], the major investments with smart grid in developing countries are presented. Even considering the investments made in developing countries, the smart grid projects are still behind in comparison to the developed ones. More recently, EVs have been seen as important DERs for the power system under this new paradigm, because they can allow bidirectional power and communication [6]. One of the main expected EV's benefits is the vehicle-to-grid (V2G) capability that will be able to support the intermittent renewable sources [10]. V2G is defined as the ability of discharging energy through the battery of the EV into the electric network. On the other hand, a large integration of DERs may turn the power system operation more complex, which will require new methodologies to deal with this challenge.

* Corresponding author. Tel.: +351 22 8340500; fax: +351 22 8321159.
E-mail address: tabsa@isep.ipp.pt (T. Sousa).
URL: http://www.gecad.isep.ipp.pt/ (T. Sousa).

http://dx.doi.org/10.1016/j.epsr.2016.03.031
0378-7796/

Nomenclature

Parameters

Δt	elementary period t duration (e.g. 15 min (0.25), 30 min (0.50))
η_c	grid-to-vehicle efficiency
η_d	vehicle-to-grid efficiency
B	imaginary part in admittance matrix [pu]
c_A	fixed component of cost function [m.u./h]
c_B	linear component of cost function [m.u./kWh]
c_C	quadratic component of cost function [m.u./kWh^2]
c	resource cost in period t [m.u./kWh]
E	stored energy in the battery of vehicle at the end of period t [kWh]
$E_{Initial}$	energy stored in the battery of vehicle at the beginning of period 1 [kWh]
E_{Trip}	energy consumption in the battery during a trip that occurs in period t [kWh]
Ex	percentage of power requirement for the AS [0–1]
G	real part in admittance matrix [pu]
N	total number of resources
Pr	percentage of power for the AS in the vehicle [0–1]
R_{AS}	active power requirement for the AS [pu]
S	maximum apparent power [pu]
T	total number of periods
TL	set of lines connected to a certain bus
$\overline{V}$	complex amplitude of voltage [pu]
W	penalization cost [m.u./kWh]
$\overline{y}$	series admittance of line that connect two buses [pu]
$\overline{y_{sh}}$	shunt admittance of line that connect two buses [pu]

Variables

θ	voltage angle
P	active power [pu]
Q	reactive power [pu]
$RLXD$	relaxation variable for down [pu]
$RLXU$	relaxation variable for up [pu]
V	voltage magnitude [pu]
X	binary variable

Indices

AS	power scheduled that will happen if the upward services (RU, SP and NS) are scheduled
$BatMax$	battery energy capacity
$BatMin$	minimum stored energy to be guaranteed at the end of period t
Bus	bus
Ch_AS	charge process for the ancillary services
Ch_ES	charge process for the energy service
D	power demand
Dch_AS	discharge process for the ancillary services
Dch_ES	discharge process for the energy service
Deg	battery degradation
DG	distributed generation unit
DG_AS	distributed generation for the ancillary services
DG_ES	distributed generation for the energy service
EV	electric vehicle
G	power generation
GCP	generation curtailment power
i, j	bus i and bus j
L	load
Max	upper bound limit
Min	lower bound limit
net_res	transition reserved capacity to be used in ancillary services
NSD	non-supplied demand
$RLXD$	relaxation variable for down
$RLXU$	relaxation variable for up
$Stored\_RD$	stored energy in the battery of the vehicle for the energy and RD services
$Stored\_RU$	stored energy in the battery of the vehicle for the energy, RU, SP and NS services
SU	external supplier
SU_AS	external supplier for the ancillary services
SU_ES	external supplier for the energy service
TFR_HV_MV	transformer that connects from high voltage to medium voltage
TFR_MV_LV	transformer that connects from medium voltage to low voltage
TL	thermal limit
$TotalMax$	total maximum limit for the resources considering the energy, RU, SP and NS services
$TotalMin$	total minimum limit for the resources considering the energy and RD services

For this future scenario, a proper ancillary services (AS) management with adequate levels of stability, safety, quality, reliability and competitiveness is essential to ensure the good operation of all power system networks, including the distribution network [11]. Typically, ancillary services can be divided in services for frequency control, voltage control and system restoration. The regulation down (RD), regulation up (RU), spinning reserve (SP) and non-spinning reserve (NS) are the four most common AS services in the frequency regulation [11]. Regulation up/down are described as the regulation reserve provided by a resource that can decrease/increase its actual operating level through automatic generation control from the system operator [11]. Spinning reserve is the portion of unloaded synchronized (or online) generating capacity that is immediately responsive to system frequency [11]. Non-spinning reserve is the portion of the generating capacity that is capable of being synchronized (or offline) and ramping to a specified load [11]. Currently, the services regarding frequency control are dealt at the transmission level by the transmission system operator (TSO), and the voltage control is locally managed at the distribution level. However, in this future scenario more frequency control participation at the distribution level is expected [12,13].

In this context, V2G has great potential in AS management, instead of using rapid ramping generators to match variable power demand [14]. Generators with rapid ramping may be expensive resources, and very pollutants. The V2G option will require an extra small cost that is related to the controllers and converters, some of which will be installed anyway in order to enable the smart charging control [15]. The V2G ability, along with quick battery reaction times, can turn EVs into a viable resource for helping the AS management [16]. EV owners can also gain an extra revenue from the participation in the AS markets, namely in the frequency regulation, while their vehicles are parked. Thus, system operator has more available resources to improve the system flexibility. Regulation up/down and spinning reserve are the two most promising frequency regulation services in which EVs can have a relevant participation [17]. A higher EVs participation in the regulation up/down than in the spinning reserve is expected, due to the highest price offered for this service. Non-spinning reserve is economically unsustainable for the EVs participation, because this service has a higher duration and a lower price than the other two services [17].

In the scope of smart grids, the aggregation of small-scale DERs is essential to integrate them into the power system management [7]. Thus, virtual power plant appears as an aggregator agent of small-scale DERs for representing them in the wholesale energy and reserves markets [18,19]. This aggregator agent will increase the profit of each small-scale DER in comparison with the scenario of individual DER participation in the wholesale markets. Over the past years, this aggregator agent concept has been evolved to incorporate other responsibilities, such as management, operation and control tasks of the small-scale DERs, as well as of the distribution network [20]. Therefore, virtual power player (VPP) concept has been proposed in [21] for aggregating small-scale DERs in the wholesale energy and reserves markets (similar to the virtual power plant concept) and for assuming the management and operation of the network in a competitive smart grid environment. VPPs can act in wholesale markets both like a producer and like a consumer depending on the type of aggregated resources and the day period. For instance, if the VPP aggregates many PV units, it can sell energy in the market during the day and buy energy during the night. Additionally, the VPP should manage the risk introduced by the uncertainties in the production, in the consumption and in the electric vehicles usage. Due to their characteristics, Virtual Power Players can provide different services in the markets, such as energy, ancillary services among others. Thus, the VPP should have a simultaneous strategy to determine the optimal scheduling of the DERs taking into account joint energy and AS managements, instead of individual managements of both services. The side-effect of creating this joint energy and AS management model is that the optimal scheduling problem turns into a complex optimization problem [22] for a scenario with large DERs penetration, namely EVs. On one hand, this optimization problem is hard to be addressed by deterministic techniques, because these techniques can take a large execution time for obtaining the optimal solution, as it is proven in [23]. On the other hand, the VPP has its own optimal scheduling related time constraints, namely, having a scheduling solution before the operation day is mandatory. For these reasons, metaheuristic techniques are very useful to support the VPP in the computation of a good solution with a low execution time. The author in [24] points the relevance of applying artificial intelligence techniques, namely metaheuristics, in different power system problems. A review of the metaheuristics used to solve optimization problem, like tabu search, simulated annealing (SA), genetic algorithm, particle swarm optimization and ant colony optimization can be seen in [25,26]. Moreover, far as the EVs scheduling problem is concerned, a summary regarding the more suitable metaheuristics has been elaborated in [27]. Nevertheless, metaheuristics should be adapted by adjusting different parameters and by incorporating heuristics in order to improve its performance. The final goal is solving the optimization problem under the VPP requirements, such as high solution quality and low execution time.

1.2. Literature review

For optimal integration of EVs in energy and AS management, new management methods should be thought of. In [28] a probabilistic dynamic method is proposed to determine the most suitable size of the reserves for different hours considering a scenario with high renewable penetration. In [29] the impact of EVs participation through V2G in frequency regulation of the West Denmark is investigated. The results showed that participation of conventional generators is significantly minimized by the EVs participation in the regulation up/down services. The performance of the automatic generation control in distribution network with high penetration of DERs is analyzed in [30]. Additionally, the authors in [31] present a short-term criterion for managing the automatic generation control under a scenario with intensive DERs penetration. Sortomme and El-Sharkawi [32,33] propose linear optimization algorithms to handle with the joint optimal bidding of an aggregator for several electricity markets, namely energy, regulation up/down and spinning reserve, without considering the impact of the scheduling solution in the electric network. On the other hand, Rotering and Ilic [34] propose a dynamic programming formulation for the EVs charging management in frequency regulation, which takes into account V2G as a mean of generating additional profits to the aggregator player. A coordinated control strategy for large EVs penetration involved in the regulation up/down is proposed in [35]. An overview of the joint energy and reserve market implementations is presented in [11]. Bessa and Matos [36] propose a day-ahead optimization model for bidding optimization of an EV aggregator that participates in the energy and secondary reserve AS market (or spinning reserve).

1.3. Main contributions

Although many works in the literature study the joint energy and AS scheduling, the application of this optimization problem for a VPP acting in a distribution network with a large DERs penetration, namely EVs, has not yet been addressed. Noticeable economic savings can be brought to the VPP by considering the joint scheduling instead of solving both scheduling problems separately. Additionally, the incorporation of an alternating current (AC) power flow model to validate the scheduling for the joint energy and AS management has been seldom considered till now. In the present paper, the energy resource scheduling simulated annealing (ERS^{2}A) algorithm [37] has been adapted to solve the optimal resource scheduling for the joint energy and AS management. Normally, this algorithm solved the day-ahead optimal resource scheduling for the energy service only. In this paper, the proposed methodology considers the regulation up/down, spinning and non-spinning reserve jointly with the energy service. Moreover, it is considered that the VPP manages DG units, EVs charge/discharge processes, and acquires energy from external suppliers located outside the VPP's network (upstream networks). The proposed ERS^{2}A algorithm is an evolution of the one proposed in [23,37]. In fact, the core process is similar however, due to the significant increase of the problem complexity (around 800,000 more variables and 900,000 more constraints), the mechanisms for the initial solution and for the generation of a neighbour solution were changed to solve the joint energy and AS scheduling problem in comparison to the energy-only scheduling problem in the previous works.

1.4. Paper organization

In addition to this introduction section, this paper includes Section 2, which presents the mathematical formulation of the optimal resource scheduling problem. Section 3 details the implementation of the proposed SA approach to solve the envisaged problem. A case study of a 33-bus distribution network with an intensive use of EVs and DG units is presented in Section 4. Finally, Section 5 exposes the most relevant conclusions of this paper.

2. Optimal resource scheduling formulation

The proposed joint energy and ancillary services optimal scheduling has the objective of minimizing the VPP's operation cost. This optimization problem is modelled as a mixed-integer non-linear programming problem. The objective function F can be formulated as

$$min\,F = \sum_{t=1}^{T} F_{ES(t)} + F_{AS(t)} \quad (1)$$

The cost $F_{ES(t)}$ represents all the costs related to the energy service and is determined as

$$
\begin{aligned}
F_{ES(t)} = & \sum_{DG=1}^{N_{DG}} c_{A(DG,t)} \times X_{DG\_ES(DG,t)} + c_{B(DG,t)} \times P_{DG\_ES(DG,t)} \\
& + c_{C(DG,t)} \times P^2_{DG\_ES(DG,t)} + \sum_{SU=1}^{N_{SU}} c_{SU\_ES(SU,t)} \times P_{SU\_ES(SU,t)(SU,t)} \\
& + \sum_{EV=1}^{N_{EV}} \left(c_{Dch\_ES(EV,t)} + c_{Deg(EV)}\right) \times P_{Dch\_ES(EV,t)} \\
& - c_{Ch\_ES(EV,t)} \times P_{Ch\_ES(EV,t)} + \sum_{DG=1}^{N_{DG}} c_{GCP(DG,t)} \times P_{GCP(DG,t)} \\
& + \sum_{L=1}^{N_L} c_{NSD(L,t)} \times P_{NSD(L,t)} \quad \forall t \in \{1, \ldots, T\}
\end{aligned} \tag{2}
$$

where external suppliers cost ($c_{SU\_ES(SU,t)}$) is considered, DG units cost (photovoltaic (PV), wind, hydro, combined heat and power (CHP), biomass, waste-to-energy (WTE) and fuel cell) being also included in $F_{ES(t)}$. EVs are also considered with a cost for the discharge process ($c_{Dch\_ES(EV,t)}$), a benefit from the charge process ($c_{Ch\_ES(EV,t)}$), and the battery degradation cost associated with additional cycling ($c_{Deg(EV)}$) [38]. Besides those costs, the costs $c_{NSD(L,t)}$ and $c_{GCP(DG,t)}$ that are related to non-supplied demand (NSD) and generation curtailment power (GCP), respectively, are also incorporated. These two costs have been included in the energy cost (2) with the purpose of having a more robust mathematical formulation handling with critical situations, namely high consumer demands or high power generation from DG units based on renewable sources.

The VPP cost for the AS markets is represented by $F_{AS(t)}$ in (1) and is given by

$$
\begin{aligned}
F_{AS(t)} \\
= & \sum_{k=1}^{4} \left(\sum_{SU=1}^{N_{SU}} c_{SU\_AS(SU,k,t)} \times P_{SU\_AS(SU,k,t)} \right. \\
& + \sum_{DG=1}^{N_{DG}} c_{DG\_AS(DG,k,t)} \times P_{DG\_AS(DG,k,t)} \\
& + W_{RLXU} \times RLXU_{(k,t)} + W_{RLXD} \times RLXD_{(k,t)} \\
& + \sum_{EV=1}^{N_{EV}} [(c_{Dch\_AS(EV,k,t)} + c_{Deg(EV)}) \times P_{Dch\_AS(EV,k,t)} \\
& \left. + c_{Ch\_AS(EV,k,t)} \times P_{Ch\_AS(EV,k,t)}] \right) \quad \forall t \in \{1, \ldots, T\}
\end{aligned} \tag{3}
$$

where the index k represents the four ancillary services going from 1 to 4 for representing the RD, RU, SP and NS, respectively. The costs with external suppliers, DG units and EVs discharge and charge processes are considered. Additionally, the relaxation variables, for up and down, $RLXU_{(k,t)}$ and $RLXD_{(k,t)}$, respectively, are activated if the resources cannot satisfy the requirement of each AS service. These variables allow the AS dispatch to be feasible in cases where the resources fail to meet the AS requirements.

The minimization of the objective function (1) leads to the minimization of the VPP operation cost for the joint energy and AS scheduling. The obtained solution must be subjected to an accurate model of the network with the purpose of verifying if it represents a feasible scheduling in the distribution network. The proposed optimal resource scheduling formulation considers an AC power flow model [39] to obtain the power flow and voltage magnitude in the distribution network buses, therefore allowing for congestion verification. The application of the Kirchhoff's current law in each bus leads for the active power to

$$
\begin{aligned}
& P_{G(i,t)} + P_{net\_res(i,t)} - P_{D(i,t)} \\
& \quad = G_{ii} \times V^2_{i(t)} + V_{i(t)} \times \sum_{j \in TL^i} V_{j(t)} \times (G_{ij} \cos\theta_{ij(t)} + B_{ij} \sin\theta_{ij(t)}) \\
& P_{G(i,t)} = \sum_{DG=1}^{N^i_{DG}} (P^i_{DG\_ES(DG,t)} - P^i_{GCP(DG,t)}) \\
& \qquad + \sum_{SU=1}^{N^i_{SU}} P^i_{SU\_ES(SU,t)} + \sum_{EV=1}^{N^i_{EV}} P^i_{Dch\_ES(EV,t)} \\
& P_{D(i,t)} = \sum_{L=1}^{N^i_L} (P^i_{L(L,t)} - P^i_{NSD(L,t)}) + \sum_{EV=1}^{N^i_{EV}} P^i_{Ch\_ES(EV,t)} \\
& \quad \forall t \in \{1, \ldots, T\}; \quad \forall i \in \{1, \ldots, N_{Bus}\}; \quad \theta_{ij(t)} = \theta_{i(t)} - \theta_{j(t)}
\end{aligned} \tag{4}
$$

where the power injected in bus i is defined as the sum of the power flow through the lines that connect this bus to the others. This injected power is equal to $P_{G(i,t)}$ plus $P_{net\_res(i,t)}$ minus $P_{D(i,t)}$ in each bus. $P_{G(i,t)}$ corresponds to the power generation that is expected to be scheduled in the energy service. $P_{net\_res(i,t)}$ is the reserved transition capacity to be used in ancillary services. This variable will establish the maximum reserved transition capacity for the network to support the possible use of reserve power in the ancillary services, in particular the upward services related to RU, SP and NS. Therefore $P_{AS(i,t)}$ will be lower or equal to $P_{net\_res(i,t)}$

$$
\begin{aligned}
& P_{AS(i,t)} \le P_{net\_res(i,t)} \\
& P_{AS(i,t)} = \sum_{k=2}^{4} \left(\sum_{DG=1}^{N^i_{DG}} P^i_{DG\_AS(DG,k,t)} + \sum_{SU=1}^{N^i_{SU}} P^i_{SU\_AS(SU,k,t)} \right. \\
& \qquad \left. + \sum_{EV=1}^{N^i_{EV}} [P^i_{Dch\_AS(EV,k,t)} + P^i_{Ch\_AS(EV,k,t)}] - R_{AS(i,k,t)} \right)
\end{aligned} \tag{5}
$$

where $P_{AS(i,t)}$ is the reserve power to be scheduled in the upward services (RU, SP and NS), if needed. The upward services are services used to increase (or upward) the generation for supporting the same increase in the demand. Variable $R_{AS(i,k,t)}$ contains the amount of active power requirement for each ancillary service k. $P_{D(i,t)}$ corresponds to the power demand that is expected to be consumed in the energy service. $P_{net\_res(i,t)}$ can be different for each bus and period, because the network can have areas with different magnitudes of congestion problems (related to voltage and line thermal limits). In more problematic areas, $P_{net\_res(i,t)}$ can be lower, therefore avoiding that the mobilization of $P_{AS(i,t)}$ (when it is necessary) is responsible for congestion problems.

It is noteworthy that AS are power reserved in day-ahead for imbalance cases in real-time. So, this power is only transformed in energy in the balancing stage. However, AS should be used in (4) to determine if their hypothetical use will cause any congestion in the power flow. The worst scenario is the one where all the upward services are activated in the balancing stage. This scenario should be used in power flow to prevent network violations that could occur when all the upward reserve is used, improving the robustness of the system. The RD service is not included in the power flow equation, because this service is characterized as an AS service for downward generation in result of an equal decrease in the demand. If RD was considered in the power flow equation, the power flow would decrease, thereby reducing the congestion and allowing generation increasing in congested areas of the network. Another important aspect in (4) is variable $P^{i}_{Ch\_AS(EV,k,t)}$ which assumes a positive value, being seen as generation resource, because it is a reduction in the upward services (RU, SP and NS) of the charge power in the energy service $P^{i}_{Ch\_ES(EV,t)}$.

For the reactive power, the current law is formulated as

$$\sum_{DG=1}^{N^{i}_{DG}} Q^{i}_{DG(DG,t)} + \sum_{SU=1}^{N^{i}_{SU}} Q^{i}_{SU(SU,t)} - \sum_{L=1}^{N^{i}_{L}} (Q^{i}_{L(L,t)} - Q^{i}_{NSD(L,t)}) = V_{i(t)} \times \sum_{j\ \in\ TL^{i}} V_{j(t)} \times (G_{ij} \sin\theta_{ij(t)} + B_{ij}\cos\theta_{ij(t)}) - B_{ii} \times V^{2}_{i(t)}$$
$$\forall t \in \{1,\ldots,T\};\quad \forall i \in \{1,\ldots,N_{Bus}\};\quad \theta_{ij(t)} = \theta_{i(t)} - \theta_{j(t)} \qquad (6)$$

For a feasible solution in terms of AC power flow, it is necessary to keep the voltage magnitude and angle under its maximum and minimum limits.

$$V^{i}_{Min} \le V_{i(t)} \le V^{i}_{Max};\quad \forall t \in \{1,\ldots,T\} \qquad (7)$$

Such as for the voltage angle bounds.

$$\theta^{i}_{Min} \le \theta_{i(t)} \le \theta^{i}_{Max};\quad \forall t \in \{1,\ldots,T\} \qquad (8)$$

A slack bus is previously selected in the network, and the reference voltage magnitude and angle are specified for it, typically is 1 and 0 for the reference voltage magnitude and angle. In the distribution network, the upper and lower bounds for voltage magnitude are typically 0.95 and 1.05.

Another important aspect to incorporate in the mathematical formulation is the constraint regarding the power flow in the line (connecting bus i to bus j) that must be lower than a maximum limit (line thermal limit)

$$\left|\overline{V_{i(t)}} \times \left[\overline{y_{ij}} \times \left(\overline{V_{i(t)}} - \overline{V_{j(t)}}\right) + \overline{y_{sh(i)}} \times \overline{V_{i(t)}}\right]^{*}\right| \le S^{max}_{TL}$$
$$\forall t \in \{1,\ldots,T\};\quad \forall i,j \in \{1,\ldots,N_{Bus}\};\quad i \ne j;\quad \forall TL \in \{1,\ldots,N_{TL}\} \qquad (9)$$

where the term $\bar{V}$ represents the voltage phasor.

The distribution network is connected to upstream networks through transformers that adapt the voltage level from high voltage (HV) to medium voltage (MV). Therefore, the external suppliers exchange energy with the VPP through these transformers, which results in a constraint regarding to the upper limit imposed by transformers' maximum capacity:

$$\left(\sum_{SU=1}^{N^{i}_{SU}} P^{i}_{SU\_ES(SU,t)} + \sum_{k=2}^{4} P^{i}_{SU\_AS(SU,k,t)}\right)^{2} + \left(\sum_{SU=1}^{N^{i}_{SU}} Q^{i}_{SU(SU,t)}\right)^{2} \le \left(S^{Max}_{TFR\_HV\_MV(i)}\right)^{2}\quad \forall t \in \{1,\ldots,T\}\ ;\forall i \in \{1,\ldots,N_{Bus}\} \qquad (10)$$

The same applies to the buses in the distribution network. There is a transformer from MV to low voltage (LV) that connects small resources, such as PV units and EVs, to the MV side

$$(P_{TFR\_MV\_LV})^{2} + (Q_{TFR\_MV\_LV})^{2} \le \left(S^{Max}_{TFR\_MV\_LV(i)}\right)^{2}$$
$$\forall t \in \{1,\ldots,T\};\quad \forall i \in \{1,\ldots,N_{Bus}\} \qquad (11)$$

where $P_{TFR\_MV\_LV(i,t)}$ and $Q_{TFR\_MV\_LV(i,t)}$ refers to the active and reactive power that flows in the MV/LV transformer, respectively:

$$P_{TFR\_MV\_LV(i,t)} = \sum_{DG=1}^{N^{i}_{DG}} \left(P^{i}_{DG\_ES(DG,t)} - P^{i}_{GCP(DG,t)} + \sum_{k=2}^{4} P^{i}_{DG\_AS(DG,k,t)}\right) + \sum_{EV=1}^{N^{i}_{EV}} \left(P^{i}_{Dch\_ES(EV,t)} - P^{i}_{Ch\_ES(EV,t)} + \sum_{k=2}^{4} (P^{i}_{Dch\_AS(EV,t)} + P^{i}_{Ch\_AS(EV,t)})\right) - \sum_{L=1}^{N^{i}_{L}} (P^{i}_{Load(L,t)} - P^{i}_{NSD(L,t)}) + \sum_{k=2}^{4} R_{AS(i,k,t)} \qquad (12)$$

$$Q_{TFR\_MV\_LV(i,t)} = \sum_{DG=1}^{N^{i}_{DG}} Q^{i}_{DG(DG,t)} - \sum_{L=1}^{N^{i}_{L}} \left(Q^{i}_{Load(L,t)} - Q^{i}_{NSD(L,t)}\right) \qquad (13)$$

The $R_{AS(i,k,t)}$ depends on a percentage of the consumers' demand plus the difference of charge and discharge of the EVs in the energy service, as described in

$$R_{AS(i,k,t)} = Ex_{(k)} \times \left(\sum_{L=1}^{N^{i}_{L}} P^{i}_{L(L,t)} + \sum_{EV=1}^{N^{i}_{EV}} P^{i}_{Ch\_ES(EV,t)} - \sum_{EV=1}^{N^{i}_{EV}} P^{i}_{Dch\_ES(EV,t)}\right);$$
$$\forall t \in \{1,\ldots,T\};\quad \forall k = \{1,2,3,4\} \qquad (14)$$

where $Ex_{(k)}$ corresponds to the percentage of power requirement for each ancillary service k. One of the main criteria to establish $Ex_{(k)}$ is through the expected power demand [40].

Then, this requirement is supported by external suppliers, DG units and EVs for the ancillary services:

$$\sum_{i=1}^{N_{Bus}} R_{AS(i,k,t)} = \sum_{DG=1}^{N_{DG}} P_{DG\_AS(DG,k,t)} + \sum_{SU=1}^{N_{SU}} P_{SU\_AS(SU,k,t)} + \sum_{EV=1}^{N_{EV}} (P_{Dch\_AS(EV,k,t)} + P_{Ch\_AS(EV,k,t)}) - RLXU + RLXD;$$
$$\forall t \in \{1,\ldots,T\};\quad \forall i \in \{1,\ldots,N_{Bus}\};\quad \forall k = \{1,2,3,4\} \qquad (15)$$

The minimum and maximum active power generation provided by the DG units for energy and AS services are formulated as

$$P_{Min(DG,t)} \times X_{DG\_ES(DG,t)} \le P_{DG\_ES(DG,t)} \le P_{Max(DG,t)} \times X_{DG\_ES(DG,t)};$$
$$\forall t \in \{1,\ldots,T\};\quad \forall DG \in \{1,\ldots,N_{DG}\} \qquad (16)$$

$$P_{Min(DG,k,t)} \le P_{DG\_AS(DG,k,t)} \le P_{Max(DG,k,t)};$$
$$\forall t \in \{1,\ldots,T\};\quad \forall DG \in \{1,\ldots,N_{DG}\} \qquad (17)$$

Additionally, the sum of the active power generation for the energy, RU, SP and NS services must be lower or equal to the power capacity of the DG unit in order to guarantee that the total generation for these services will not violate the maximum power generated by the DG unit

$$P_{DG\_ES(DG,t)} + \sum_{k=2}^{4} P_{DG\_AS(DG,k,t)} \le P_{TotalMax(DG,t)} \times X_{DG\_ES(DG,t)}$$
$$\forall t \in \{1,\ldots,T\};\quad \forall DG \in \{1,\ldots,N_{DG}\} \tag{18}$$

On the other hand, it is necessary to include a constraint that establishes the difference between the active power generation for the energy and RD services. The RD service is a reduction in the power generation to the scheduled generation in the energy service of the *DG* unit. The scheduled power must be higher or equal to the minimum generation power limit

$$P_{DG\_ES(DG,t)} - P_{DG\_AS(DG,k,t)} \ge P_{TotalMin(DG,t)} \times X_{DG\_ES(DG,t)}$$
$$\forall t \in \{1,\ldots,T\}; \forall DG \in \{1,\ldots,N_{DG}\};\quad \forall k = 1 \tag{19}$$

The minimum and maximum reactive power generation limits that each DG unit can provide are given by

$$Q_{Min(DG,t)} \le Q_{DG(DG,t)} \le Q_{Max(DG,t)};$$
$$\forall t \in \{1,\ldots,T\};\quad \forall DG \in \{1,\ldots,N_{DG}\} \tag{20}$$

In the distribution network, most of the DG units use asynchronous generators that only generate active power with capacitor banks to produce reactive power. For the case of PV units, an inverter is used to convert the power generation from DC to AC. Therefore, active and reactive power generation can be separated in several equations with their own upper and lower bounds, as can be found in [41].

The maximum active power generation provided by the external supplier for all services is defined as

$$P_{SU\_ES(SU,t)} \le P_{Max(SU,t)};\quad \forall t \in \{1,\ldots,T\};\quad \forall SU \in \{1,\ldots,N_{SU}\} \tag{21}$$

$$P_{SU\_AS(SU,k,t)} \le P_{Max(SU,k,t)};$$
$$\forall t \in \{1,\ldots,T\};\quad \forall SU \in \{1,\ldots,N_{SU}\};\quad k \in \{1,2,3,4\} \tag{22}$$

Moreover, the external suppliers need to consider the same type of conditions as the ones formulated by constraints (18) and (19) for the DG units:

$$P_{SU\_ES(SU,t)} + \sum_{k=2}^{4} P_{SU\_AS(SU,k,t)} \le P_{TotalMax(SU,t)};$$
$$\forall t \in \{1,\ldots,T\};\quad \forall SU \in \{1,\ldots,N_{SU}\} \tag{23}$$

$$P_{SU\_ES(SU,t)} - P_{SU\_AS(SU,k,t)} \ge 0;$$
$$\forall t \in \{1,\ldots,T\};\quad \forall SU \in \{1,\ldots,N_{SU}\};\quad \forall k = 1 \tag{24}$$

Finally, for each external supplier *SU*, it is necessary to maintain the reactive power generation below its maximum limit, as described in

$$Q_{SU(SU,t)} \le Q_{Max(SU,t)};\quad \forall t \in \{1,\ldots,T\};\quad \forall SU \in \{1,\ldots,N_{SU}\} \tag{25}$$

In regulation down, EVs need to increase their power charge or to decrease their power discharge in comparison to their operation level scheduled in the energy service ($P_{Ch\_ES(EV,t)}$ and $P_{DCh\_EV(EV,t)}$), because it is an AS for downward generation. On the other hand, EVs need to decrease their power charge or to increase their power discharge for the regulation up, spinning reserve and non-spinning reserve, because these services represent the AS for upward generation. Therefore, the upward and downward generation cannot occur at the same time, but it is possible to have different scenarios for the AS requirements in the next day. For instance, a scenario that considers the upward and downward generation in alternate periods is possible to occur, as well as another scenario that requires the downward generation in the off-peak periods and the upward generation in the peak periods is also possible. Thus, it is possible to establish the next scenarios as the two most critical scenarios in the next day: (1) when it is required AS for downward generation (i.e. RD) during all periods; (2) when it is necessary to use AS for upward generation (i.e. RU, SP and NS) during all periods. These two scenarios will have a large impact in the EV battery than other less stressful scenarios for AS requirements. For this reason, considering the management of the energy stored in the EV batteries in these two critical scenarios is mandatory.

Starting by the RU, SP and NS services (upward generation services), the energy stored in the battery in each period *t* is calculated as

$$\begin{aligned} &E_{Stored\_RU(EV,t)} \\ &= E_{Stored\_RU(EV,t-1)} - E_{Trip(EV,t)} + \Delta t \times \eta_{c(EV)} \\ &\quad \times \left(P_{Ch\_ES(EV,t)} - \sum_{k=2}^{4} P_{Ch\_AS(EV,k,t)} \right) \\ &\quad - \Delta t \times \frac{1}{\eta_{d(EV)}} \times \left(P_{Dch\_ES(EV,t)} + \sum_{k=2}^{4} P_{Dch\_AS(EV,k,t)} \right) \\ &t = 1 \rightarrow E_{Stored\_RU(EV,t-1)} = E_{Initial(EV)}; \\ &\forall t \in \{1,\ldots,T\};\quad \forall EV \in \{1,\ldots,N_{EV}\} \end{aligned} \tag{26}$$

where $E_{Trip(EV,t)}$ stands for the typical daily driving pattern of each user. This variable will cause a decrease in the energy stored of the battery when the vehicle is travelling. Thus, the VPP must guarantee that the EV has the required amount of energy stored in the battery for supporting the driving pattern in the time horizon of the optimal resource scheduling problem. The driving pattern can be sent by the EV owner [42] or a forecast tool [43], or an optimization approach [44] can be used, to predict the EVs owners behaviour. From this information, it is possible to know how much expected energy is necessary to charge the EV, taking into account the EV owner driving pattern.

This energy stored in the AS for upward generation must be under a maximum and minimum energy limit for all periods

$$E_{BatMin(EV,t)} \le E_{Stored\_RU(EV,t)} \le E_{BatMax(EV,t)};$$
$$\forall t \in \{1,\ldots,T\};\quad \forall EV \in \{1,\ldots,N_{EV}\} \tag{27}$$

where $E_{BatMax(EV,t)}$ corresponds to the battery capacity and $E_{BatMin(EV,t)}$ corresponds to the minimum amount of energy stored that the EV user wants in a particular period.

The power charge for the RU, SP and NS must be lower or equal to the power charge in the energy service, because it is seen as a reduction of the power charge in the energy service:

$$P_{Ch\_ES(EV,t)} \ge \sum_{k=2}^{4} P_{Ch\_AS(EV,k,t)};$$
$$\forall t \in \{1,\ldots,T\};\quad \forall EV \in \{1,\ldots,N_{EV}\} \tag{28}$$

In addition, the power discharge from the energy, RU, SP and NS services must be lower or equal to the maximum discharge power limit, because the discharge in the RU, SP and NS is an extra power generation:

$$P_{Dch\_ES(EV,t)} + \sum_{k=2}^{4} P_{Dch\_AS(EV,k,t)} \le P_{Max(EV,t)}; \quad \forall t \in \{1,\ldots,T\}; \quad \forall EV \in \{1,\ldots,N_{EV}\} \tag{29}$$

Regarding the RD service (downward generation service), the energy stored is also necessary to determine

$$\begin{aligned} E_{Stored\_RD(EV,t)} &= E_{Stored\_RD(EV,t-1)} - E_{Trip(EV,t)} + \Delta t \times \eta_{c(EV)} \\ &\quad \times (P_{Ch\_ES(EV,t)} + P_{Ch\_AS(EV,k,t)}) \\ &\quad - \Delta t \times \frac{1}{\eta_{d(EV)}} \times (P_{Dch\_ES(EV,t)} - P_{Dch\_AS(EV,k,t)}) \\ &\quad t = 1 \rightarrow E_{Stored\_RD(EV,t-1)} = E_{Initial(EV)}; \\ &\quad \forall t \in \{1,\ldots,T\}; \quad \forall EV \in \{1,\ldots,N_{EV}\}; \quad k = 1 \end{aligned} \tag{30}$$

For this service, ensuring that the energy stored is under its maximum and minimum limits is also needed

$$E_{BatMin(EV,t)} \le E_{Stored\_RD(EV,t)} \le E_{BatMax(EV,t)}; \quad \forall t \in \{1,\ldots,T\}; \quad \forall EV \in \{1,\ldots,N_{EV}\} \tag{31}$$

The power charge for the energy plus the RD service ($k = 1$) must be lower or equal to the maximum power charge limit, as described by

$$P_{Ch\_ES(EV,t)} + P_{Ch\_AS(EV,k,t)} \le P_{Max(EV,t)}; \quad \forall t \in \{1,\ldots,T\}; \quad \forall EV \in \{1,\ldots,N_{EV}\}; \quad k = 1 \tag{32}$$

Then, the power discharge from the RD service ($k = 1$) must be lower or equal to the power discharge from the energy service that is given by

$$P_{Dch\_ES(EV,t)} \ge P_{Dch\_AS(EV,k,t)}; \quad \forall t \in \{1,\ldots,T\}; \quad \forall EV \in \{1,\ldots,N_{EV}\}; \quad k = 1 \tag{33}$$

The power charge and discharge for the energy service must be lower or equal to their own maximum limit:

$$P_{Ch\_ES(EV,t)} \le P_{Max(EV,t)} \times X_{Ch\_ES(EV,t)}; \quad \forall t \in \{1,\ldots,T\}; \quad \forall EV \in \{1,\ldots,N_{EV}\} \tag{34}$$

$$P_{Dch\_ES(EV,t)} \le P_{Max(EV,t)} \times X_{Dch\_ES(EV,t)}; \quad \forall t \in \{1,\ldots,T\}; \quad \forall EV \in \{1,\ldots,N_{EV}\} \tag{35}$$

The maximum charge and discharge limits, respectively, for the AS need also to be considered:

$$P_{Ch\_AS(EV,k,t)} \le Pr_{AS(EV,k)} \times P_{Max(EV,t)} \times X_{Ch\_AS(EV,k,t)} \tag{36}$$

$$P_{Dch\_AS(EV,k,t)} \le Pr_{AS(EV,k)} \times P_{Max(EV,t)} \times X_{Dch\_AS(EV,k,t)} \quad \forall t \in \{1,\ldots,T\}; \quad \forall EV \in \{1,\ldots,N_{EV}\}; \quad k = \{1,2,3,4\} \tag{37}$$

where $Pr_{AS(EV,k)}$ is the percentage of maximum limit that can be used in the charge and discharge processes.

It is also important to guarantee that charge and discharge do not occur in the same period for the energy and AS services, respectively, this being defined as

$$X_{Ch\_ES(EV,t)} + X_{Dch\_ES(EV,t)} \le 1 \tag{38}$$

$$\begin{aligned} &X_{Ch\_AS(EV,k,t)} + X_{Dch\_AS(EV,k,t)} \le 1; \\ &\quad \forall t \in \{1,\ldots,T\}; \quad \forall EV \in \{1,\ldots,N_{EV}\} \\ &X_{Ch\_ES(EV,t)} \text{ and } X_{Dch\_ES(EV,t)} \in \{0,1\}; \\ &X_{Ch\_AS(EV,k,t)} \text{ and } X_{Dch\_AS(EV,k,t)} \in \{0,1\} \end{aligned} \tag{39}$$

3. Simulated annealing approach

The present section describes the proposed ERS^{2}A methodology implemented to determine the day-ahead optimal resource scheduling for the energy and AS joint management considering the mathematical formulation presented in the previous section.

3.1. Simulated annealing principles

The simulated annealing algorithm was proposed in 1983 by Kirkpatrick et al. [45] and Laarhoven and Aarts [46]. Since then, the SA algorithm has been used with success to solve hard and complex problems in many applications [47,48]. The main advantages of the SA algorithm over population based metaheuristics (e.g. genetic algorithm, particle swarm optimization and ant colony optimization) are its simplicity and its need for less computational resources (memory and time). Nevertheless, a good computational performance of the SA algorithm will be achieved through the development of heuristics for obtaining a good initial solution [23,37] and the parameterization of its parameters.

The SA algorithm is based on the cooling process seen in metallurgy, in which the algorithm simulates the heat process of a metal, followed by the cooling process that reduces the temperature until the metal achieves a crystallized state [49]. The generic SA algorithm starts with a random initial solution, and then a neighbourhood scheme is used to obtain neighbour solutions. In the generic SA algorithm, a random neighbour solution is selected, but there are specific applications in which the SA only generates a single neighbour [23]. If the neighbour solution is better than the current solution, then the neighbour will be used for the next iteration. Otherwise, the neighbour can be also accepted based on the Boltzmann probability [45]:

$$p = e^{-((|F_W - F_C|)/T_K)} \tag{40}$$

where T_K is the temperature value at iteration K, F_W and F_C are the fitness function value of the neighbour and current solution, respectively.

If this probability is higher than a random value, then the neighbour will be used in the next iteration. This second step will enable the SA algorithm to accept a worse solution to avoid local optima. For this reason, the temperature parameter starts at high level in the beginning of the SA algorithm. The temperature will control the behaviour of the Boltzmann probability, and typically at the beginning, the SA algorithm will accept easily worse neighbour solutions than at the end of the iterative process, due to the reduction of the temperature value. This temperature reduction is achieved from a cooling scheduling that decreases the temperature value during the iterative process. The SA algorithm will stop if the maximum number of iterations is achieved or if the temperature overtakes a minimum value or if other criterion is reached.

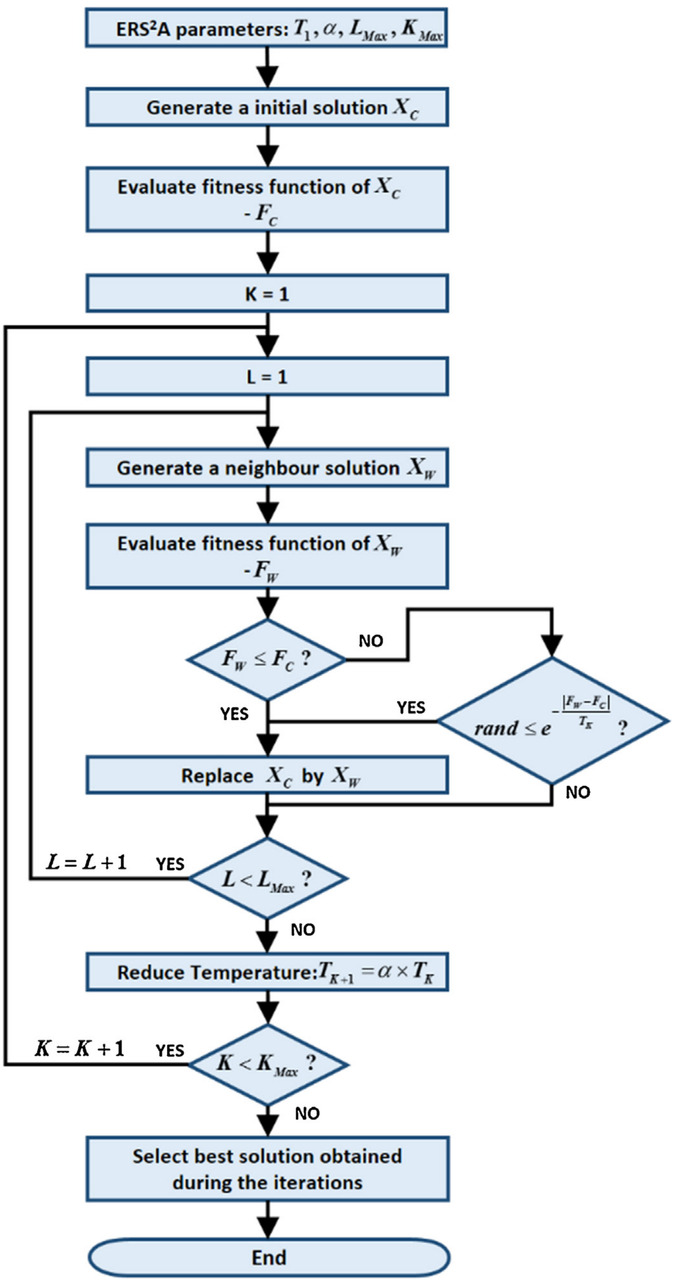

Fig. 1. Flowchart of the ERS²A algorithm for the optimal resource scheduling considering energy and AS.

3.2. Proposed simulated annealing

The ERS²A algorithm proposed in [37] has been adapted in this paper for taking into account the joint energy and AS scheduling problem. As mentioned in the introduction section, ERS²A was primarily developed to solve the day-ahead optimal resource scheduling for the energy service considering an intensive use of electric vehicles. Fig. 1 illustrates the flowchart of the ERS²A algorithm adapted in this paper.

First, the initial temperate value (T_1), the cooling rate value (α), the maximum number of iterations at same temperature (L_{Max}) and the maximum number of iterations (K_{Max}) are initialized in the ERS²A algorithm. Next, the initial solution of ERS²A (X_C) is obtained through the use of two heuristics, designated as naive EVs charge and discharge allocation (NECA) and generation tournament based cost (GETCO). A more detailed description of these two heuristics can be found in [37]. Nevertheless, a brief explanation is hereby given. NECA heuristic is used to allocate EVs charge in periods with low demand (off-peak periods) and EVs discharge in periods with high demand (peak periods). NECA heuristic guarantees an initial solution for the charge and discharge of EVs in the energy service without constraint violations (26)–(39). The violations in these constraints are avoided, because the new charges and discharges for each EV are randomly generated between two bounds: (i) lower one is zero; and (ii) upper one is the minimum value between the maximum charge/discharge limit and the energy difference (ΔE). ΔE is the difference between the energy stored in the battery at the last period and the minimum energy limit. When ΔE is higher than zero, this means that NECA can generate a discharge value in a peak period, because the vehicle has more energy in the battery than required by the user for a trip. Then, NECA moves to a new vehicle to generate a solution. If ΔE is lower than zero, this means that NECA needs to generate a charge value in an off-peak period, because there is not enough energy in the battery to support the vehicle's trips. This process will continue until ΔE is higher or equal to zero in order to guarantee enough energy to support the vehicle's trips.

Afterwards, a heuristic is incorporated in the ERS²A algorithm to stimulate the EVs scheduling in peak periods for the RD, RU and SP services, instead of using expensive resources in AS during these periods. Charge or discharge will be selected based on the lowest price for the VPP. As mentioned before, EVs will not participate in the non-spinning reserve service, because it is economically unsustainable for EVs. Then, GETCO mechanism is applied to schedule generation resources (DG units and external suppliers) after knowing the scheduling of EVs. Basically, this heuristic uses a tournament to dispatch the generation resources considering the average cost of each resource, resulting in the scheduling of the resources with the lowest cost. GETCO mechanism jointly dispatches the generation resources for both the energy and AS services.

The inclusion of these heuristics in the initial solution is important to give a good initial point in the ERS²A algorithm, instead of using a random movement [37]. This fact will help reducing the computational effort (CPU time and memory) required by this kind of optimization. The heuristics used in the ERS²A algorithm guarantee an initial solution without violating the constraints related to DERs (10)–(39).

In the next step, the initial solution is evaluated through a fitness function expression (F_C) composed by the operation cost (1) plus penalizations for voltage magnitude (7), voltage angle (8) and line thermal limit (9) violations [50]. A robust AC power flow model for distribution networks from [51] is applied to ensure that the initial solution does not violate the Kirchhoff's current law in each bus (4)–(6). This power flow is executed before the fitness function evaluation of the solution and the power losses are compensated by the external suppliers or DG units that did not reach their maximum active power generation.

Afterwards, the iterative process of the ERS²A algorithm proceeds with the generation of a new neighbour solution (X_W) using the proposed heuristic in [23]. This heuristic, called intelligent EVs allocation, re-schedules EVs charge and discharge in the best periods to decrease the fitness function. The intelligent EVs allocation heuristic has been adapted in this paper to jointly re-schedule the EVs in the energy and AS services. Additionally, the mean operation cost value for each period has been included to improve this heuristic finding a better neighbour solution. This heuristic has been changed in this paper in order to obtain the re-schedules of EVs charge and discharge without violating EV constraints (26)–(39). This heuristics incorporates a similar approach as the one implemented in NECA, where the new charges and discharges for a selected period are randomly generated between two bounds: (i) lower one is the previous charge/discharge value; and (ii) upper one is the minimum value between the maximum charge/discharge limit or the extra energy that can be stored in the battery. For new charge values, this extra energy is the difference between the maximum energy limit and the energy stored in the selected period to charge. For new discharge values, this extra energy is the difference between the energy stored in the selected period to discharge and the minimum energy limit. For each vehicle, if any change in the intelligent EVs allocation heuristic leads to violations in the constraints (26)–(39) of that vehicle, the solution is not accepted and in the next iteration of ERS^{2}A the heuristic runs again to obtain a feasible one. This strategy avoids that the ERS^{2}A algorithm gets stuck in the same iteration. Then, GETCO heuristic is used to schedule the generation resources for the new neighbour solution. Moreover, constraints (10)–(39) are implicitly handled in the neighbourhood scheme in order to generate a new solution without any violations. The new neighbour solution is evaluated using the same fitness function expression (F_W) used in the initial solution. The next steps are used to accept the neighbour solution for the next iteration, if this solution is better than the initial one or if its Boltzmann probability (40) is higher than a random value. Otherwise, the initial solution will continue for the next iteration.

Then, the methodology will return to the step of generating a new neighbour solution, if L is lower or equal to the parameter L_{Max}. Otherwise, the temperature will be reduced for the next iteration (T_{K+1}) through the geometric scheme [49], as given by

$$T_{K+1} = \alpha \times T_k \tag{41}$$

The ERS^{2}A algorithm stops when the maximum number of iterations is reached, or if the fitness function does not present any improvement during a certain number of iterations (for this paper, 20 iterations have been defined). Afterwards, the best solution obtained during the iterations is selected as the final solution of the ERS^{2}A algorithm.

4. Case study

An empirical investigation for the joint management of energy and AS considering large penetration of EVs is performed in this section. A 33-bus distribution network [52] managed by a VPP has been used to test and validate the proposed ERS^{2}A methodology. In this network a high penetration of DG units to the year 2040 is considered [52]. Fig. 2 shows the 33-bus distribution network and the DG units considered in this case study (DG is identified by technology in Fig. 2).

VPP will manage this 33-bus distribution network with 66 DG units: 32 PV, 15 CHP, 8 fuel cell, 5 wind, 3 biomass, 2 small hydro and 1 WTE unit. The VPP also has the opportunity of negotiating with 10 external suppliers that can represent bilateral contracts and/or participation in electricity markets. This distribution network is connected to high voltage level (upstream network) through bus 0, and the negotiated energy from these external suppliers flows through this bus 0. A total number of 218 consumers distributed throughout 32 buses will be satisfied by the VPP, and the peak power demand is around 4.2 MW in hour 20.

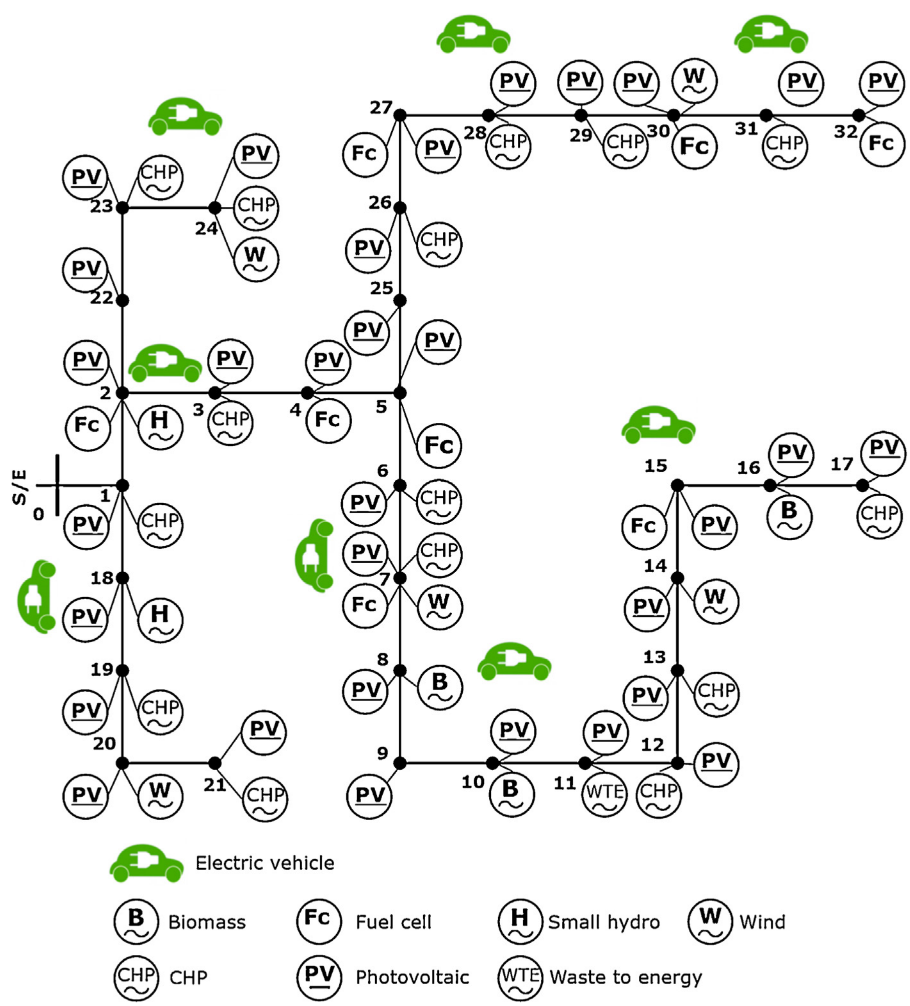

Fig. 2. 33-bus distribution network [52].

Table 1
Driving pattern of 2000 EVs.

Driving pattern	Driving stats
Trip distance (km)	
Maximum	194
Mean	57
Minimum	2.5
Total trip distance (km)	116,642
Total energy consumption (kWh)	12,479
Mean battery capacity (kWh)	16

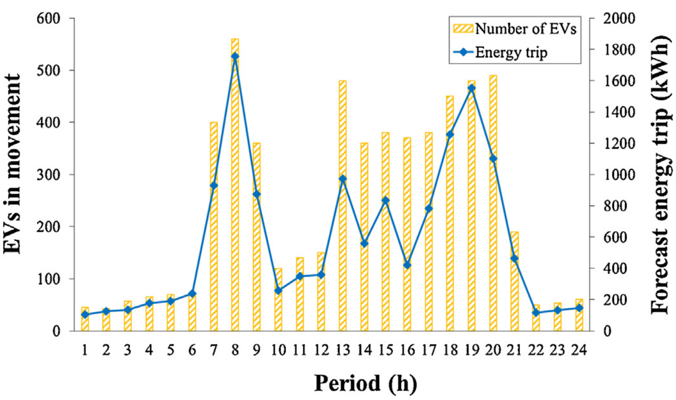

Fig. 3. Driving pattern and number of EVs in movement.

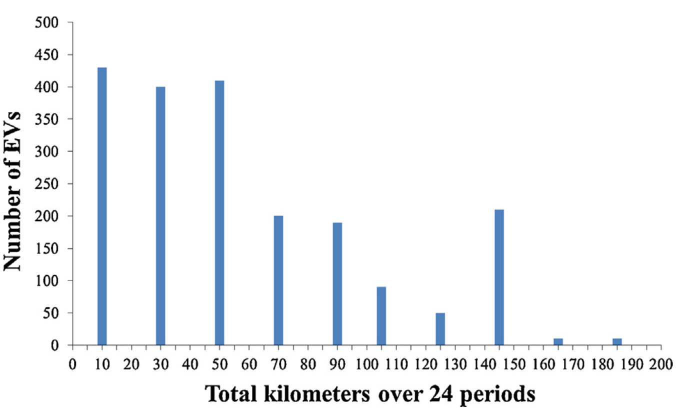

Fig. 4. Histogram of EVs total distance.

The VPP can also control the charge and discharge processes of the EVs connected to the 33-bus distribution network. In this case study, a scenario with 2000 EVs is considered, and the simulator tool proposed in [43] was used to generate the daily driving patterns for the 2000 EVs. The simulator tool considers seven commercial EV models, and the respective data can be obtained in [23]. These models are equally spread over the 2000 EVs in the case study, considering the same areas as presented in [23] for the slow and fast charge of EVs. The degradation cost of EVs (2)–(3) can be obtained using the model proposed in [53], thereby this case study considers a degradation cost of 0.03 m.u./kWh.

Table 3
Quadratic cost function for CHP, biomass and WTE units.

Resource	c_A (m.u./h)	c_B (m.u./kWh)	c_C (m.u./kWh^2)
CHP	0.005	0.1003	0.005
Biomass	0.010	0.1975	0.006
WTE	0.005	0.0549	0.003

The driving stats resulting from the use of simulator tool to generate the scenario with 2000 EVs are shown in Table 1. The mean distance travelled by EVs was around 57 km while the maximum and minimum distances were around 194 km and 2.5 km, respectively. The driving pattern generated to this case study achieved a total trip distance of approximately 116,642 km that corresponds to a total energy consumption by the EVs batteries of 12,479 kWh.

In order to simulate the movements and distance, the simulator tool used the profiles reported by the U. S. Department of Transportation in [54]. Fig. 3 shows the outcome of simulated movements during the 24 periods of the case study. The bars express the total number of EVs in movement for each period and the line corresponds to the total trip distance made in each period. EV trips are more concentrated between periods 7–9 and periods 18–20. Additionally, the histogram of the number of EVs that travel around the same distance over 24 periods is illustrated in Fig. 4.

The power supply and price of each resource for all services are presented in Tables 2–4, respectively. The total installed capacity of each resource is also available in Table 2. The VPP established "take-or-pay" contracts with the 32 photovoltaic units, resulting in the obligation of the VPP to dispatch all the energy supplied by photovoltaic units in the energy service. The wind resources only participate in the energy and regulation up/down. EVs are only used in the energy, regulation up/down and spinning reserve. Table 3 presents the fixed (c_A), linear (c_B) and quadratic (c_C) cost coefficient for the CHP, biomass and WTE units that consider the quadratic cost equation. The other DG units only consider the linear cost coefficient illustrated in Table 4.

For comparison purposes, the mathematical formulation presented in Section 2 has been implemented in mixed-integer non-linear programming (MINLP) approach (deterministic technique) using the software general algebraic modelling system (GAMS). The proposed ERS^{2}A algorithm has been developed in MATLAB software. Both approaches have been tested on a computer with two processors Intel® Xeon® E5-2620 v2 2.10 GHz, each one with two cores, 16 GB of random-access-memory and Windows 8.1 Professional 64 bits operating system.

The results of this case study will be divided into three subsections. Section 4.1 shows the results of the MINLP approach implemented in GAMS for the optimal scheduling problem considering joint energy and AS, and separated energy and AS scheduling. This subsection will prove the economic effectiveness of the

Table 2
Distributed energy resources' power capacity.

Resource	Power capacity (kW)					
	Total	Energy	Regulation down	Regulation up	Spinning reserve	Non-spinning
PV	1320	1320	–	–	–	–
Wind	505	505	50.5	50.5	–	–
Small hydro	80	80	8	8	8	8
CHP	725	725	36.25	72.5	72.5	72.5
Biomass	350	350	17.5	35	35	35
WTE	10	10	0.5	1	1	1
Fuel cell	440	440	22	44	44	44
External suppliers	2900	2900	145	145	145	290

Table 4
Distributed energy resources' bids prices.

Resource	Price (m.u./kWh)			
	Energy	Regulation up/down	Spinning reserve	Non-spinning
PV	0.1840	–	–	–
Wind	0.0720	0.0792	–	–
Small hydro	0.0655	0.0720	0.0786	0.0819
CHP	–	0.1104	0.1204	0.1254
Biomass	–	0.2172	0.2370	0.2469
WTE	–	0.0604	0.0659	0.0686
Fuel cell	0.1242	0.1367	0.1491	0.1553
External suppliers	0.1050	0.1155	0.1260	0.1313
EVs				
Charge	0	0.05	0.06	–
Discharge	0.03			

Table 5
Comparison of the results for the joint and separate management.

Optimal resource scheduling model	Energy cost (m.u.)	AS cost (m.u.)	Operation cost (m.u.)
Joint management	7634.85	982.25	8617.10
Separate management	7208.46	1822.30	9030.76

proposed joint energy and AS management. Section 4.2 depicts the comparison between the ERS^{2}A and the MINLP approaches results in the day-ahead optimal resource scheduling problem for the energy and AS joint management. In Section 4.3, the main case-study results are presented and discussed.

4.1. Comparison of the joint energy and AS with separated markets approaches

The MINLP determined the optimal resource scheduling problem for the energy and AS management, considering a joint management and a separate management. Table 5 presents the results for both managements.

The MINLP obtained an operation cost of 8617.10 m.u. for the day-ahead joint management of energy and AS. On the other hand, the separate management of the energy and AS presented a higher operation cost of 9030.76 m.u. In terms of energy cost, the joint management achieved a higher cost of 7634.85 m.u., and the separate management only obtained a cost of 7208.46 m.u. On the contrary, the AS cost of the joint management is 982.25 m.u. that is much lower than the cost of 1822.30 m.u. for separate management. The conclusion is that joint management of energy and AS helps the VPP to reduce the total operation costs, improving the system social welfare. The use of the joint management of energy and AS leads to an economic saving for the VPP of 413.66 m.u., representing around 4.6% of the separate management's operation cost. Considering that the VPP would obtain this economic saving over a year, the VPP would achieve a year's expected saving of 150,985.90 m.u. (413.66 × 365).

4.2. Comparison of the proposed SA with the deterministic approach

A sensitivity analysis of the ERS^{2}A parameters has been made with the purpose of tuning the algorithm for this case study. This algorithm performed several runs with different parameter values until the ERS^{2}A algorithm obtained a constant low value for the fitness function. For each parameter value, the ERS^{2}A has been run 100 times in order to establish if the parameter value was suitable to the case study. Table 6 shows the ERS^{2}A parameters values used for this case study.

After tuning the SA parameters, the ERS^{2}A algorithm has been used to determine the day-ahead optimal resource scheduling for the energy and AS joint management. The ERS^{2}A result has been compared with the MINLP approach. Table 7 presents the ERS^{2}A result for a total of 1000 runs for this case study. The minimum, maximum and mean operation cost as well as standard deviation are shown in this table.

Table 6
Parameters used in the proposed SA methodology.

Parameters	ERS^{2}A
Initial temperature – T_1	0.075
Cooling rate – α	0.8
Max. number of iterations – K_{Max}	50
Max. number of iterations at same temperature – L_{Max}	5
Max. number of iterations without improvements	20

The ERS^{2}A algorithm presented a maximum operation cost of 8720.52 m.u., a minimum operation cost of 8706.06 m.u., a mean operation cost of 8712.34 m.u., and a standard deviation of 2.44 m.u. It is concluded that the proposed algorithm showed a good performance with a low standard deviation, and a maximum cost closer to the minimum cost. Moreover, the ERS^{2}A algorithm exposes a robust behaviour in the 1000 trials. For this case study, the MINLP and the ERS^{2}A approaches obtained an operation cost of 8617.10 m.u. and 8706.06 m.u., respectively. The ERS^{2}A solution is closer to the MINLP results, presenting a small difference of 1.03%. Therefore, this ERS^{2}A performance encourages the application of this methodology to the day-ahead optimal resource scheduling problem for the energy and AS joint management.

In terms of execution time, the MINLP and the ERS^{2}A approaches achieved a time of 119,404 s (corresponding to 33.17 h) and 70.70 s, respectively. The ratio between the times of MINLP and ERS^{2}A approaches is about 1689. Thus, the proposed algorithm is approximately 1689 faster than the MINLP approach. Another important aspect is related to the need of VPP having a scheduling solution for the next day in less than 24 h. Therefore, ERS^{2}A algorithm presents a solution closer to the optimal one with a low execution time, on the other hand, MINLP approach is not able to present a solution in short-time (<24 h). This ERS^{2}A performance encourages the VPP to test and validate several scenarios for the next day considering different behaviours for the renewable sources (e.g. wind and solar) or EV driving patterns without losing quality in the solutions found and with a low execution time.

Fig. 5 depicts the histogram of the fitness function for 1000 runs of the ERS^{2}A algorithm. Most of the runs found a fitness function

Table 7
Comparison of the results for the proposed SA and MINLP approaches.

Method	Operation cost (m.u.)				Mean execution time (s)	Trials violation (#)
	Minimum	Maximum	Mean	Standard deviation		
MINLP	8617.10	–	–	–	119,404	–
ERS^{2}A	8706.06	8720.52	8712.34	2.44	70.70	0/1000

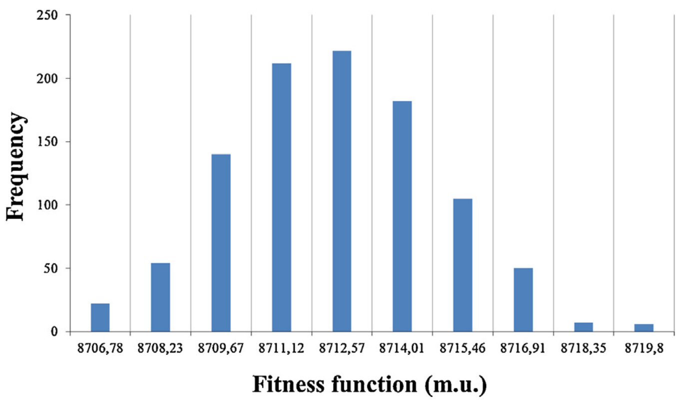

Fig. 5. Histogram of the fitness function for 1000 runs.

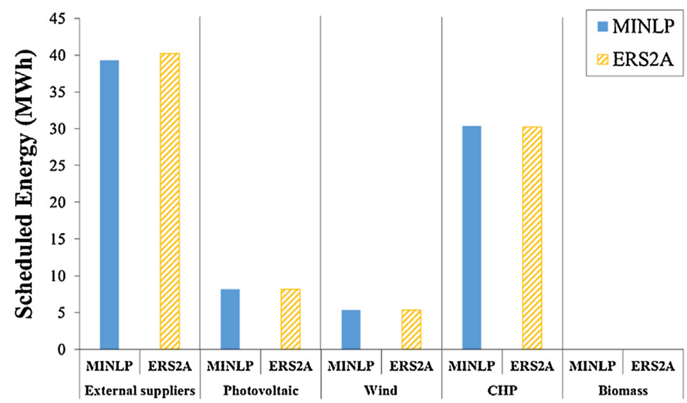

Fig. 7. Scheduled energy by external suppliers and DG in the 24 periods.

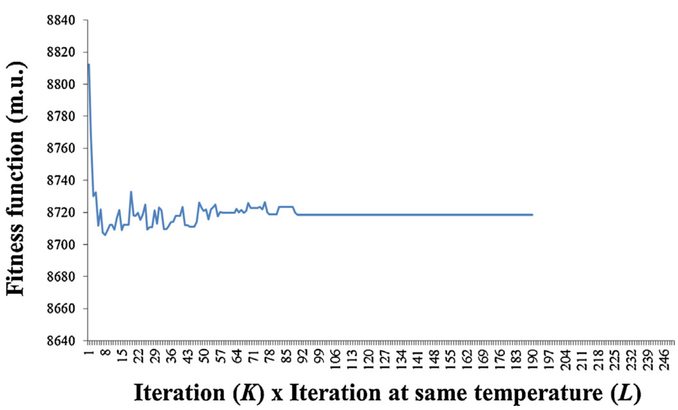

Fig. 6. Fitness function performance of the ERS^{2}A algorithm.

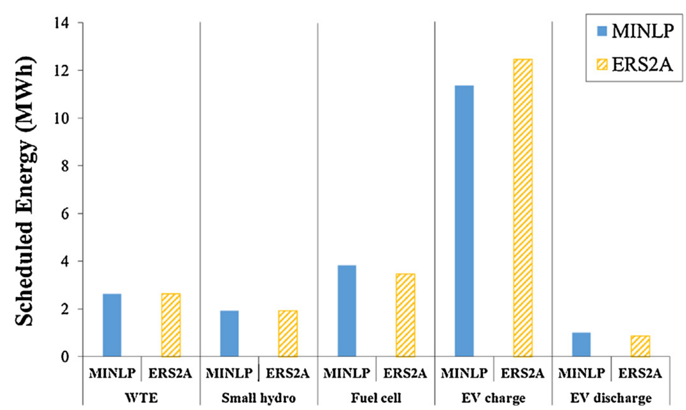

Fig. 8. Scheduled energy by DG and EV in the 24 periods.

between 8709 m.u. and 8714 m.u. proving the good consistency of the proposed SA approach to solve this optimization problem. With this histogram we can say that a new run test will fall in this range of values with high chance. In particular, a new run will have 75.6% chance of obtaining a fitness function between 8709 m.u. and 8714 m.u.

The fitness function evolution for the trial with the minimum operation cost of ERS^{2}A algorithm is presented in Fig. 6. The fitness function evolution is presented for each iteration (K) and for each iteration at same temperature (L). This algorithm presented a fast convergence (in few iterations) towards a good solution.

4.3. Case-study results

Figs. 7 and 8 depict a comparison of the results of MINLP and ERS^{2}A algorithms for the total scheduled energy for all services (energy, RD, RU, SP and NS). Fig. 7 shows the scheduled energy for the external suppliers, PV, wind, CHP and biomass units. On the other hand, Fig. 8 shows the scheduling result for the WTE, small hydro, fuel cell and EVs charge and discharge. The MINLP and ERS^{2}A algorithms achieved similar scheduling results for the PV, wind, CHP, biomass, WTE, small hydro and EVs discharge. In the case of biomass units, both algorithms scheduled them at zero due to their high cost. The biggest differences between the MINLP and the ERS^{2}A were achieved in the external suppliers, fuel cell and EVs charge. In fact, the ERS^{2}A charge more EVs than the MINLP, resulting in EVs with more energy stored in their batteries at the end of the 24 periods. For this reason, the ERS^{2}A had to schedule more external suppliers to charge more EVs.

Fig. 9 shows the energy resource scheduling of the best solution obtained by the ERS^{2}A algorithm. The blue line with squares represents the consumer demand, on the other hand, the system demand (consumer demand plus EVs charge power and active power losses) is represented by the yellow line with lozenges. The results designated as other resources correspond to the scheduling results of CHP, fuel cell, small hydro and WTE. As expected, the proposed algorithm schedules the EVs charge in the off-peak periods, because there are more available low cost generation resources (DG and external suppliers) in these periods. The EVs discharge has been scheduled in peak periods, instead of using other generation resources more expensive than electric vehicles.

Figs. 10 and 11 depict the energy resource scheduling for the regulation down and up services, respectively. In Figs. 10 and 11, other resources stand for the results obtained in WTE, small hydro and fuel cell resources. Biomass has been dispatched at zero in both RD and RU services, because of being a very expensive resource. In the RD service, the ERS^{2}A algorithm scheduled the EVs charge to

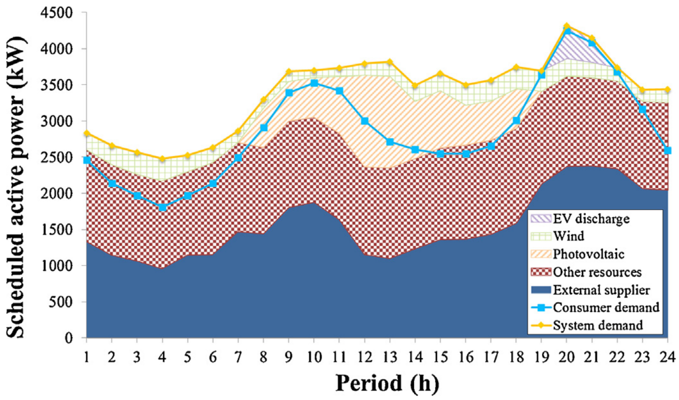

Fig. 9. Energy resource scheduling for the energy service. (For interpretation of the references to colour in this figure citation, the reader is referred to the web version of this article.)

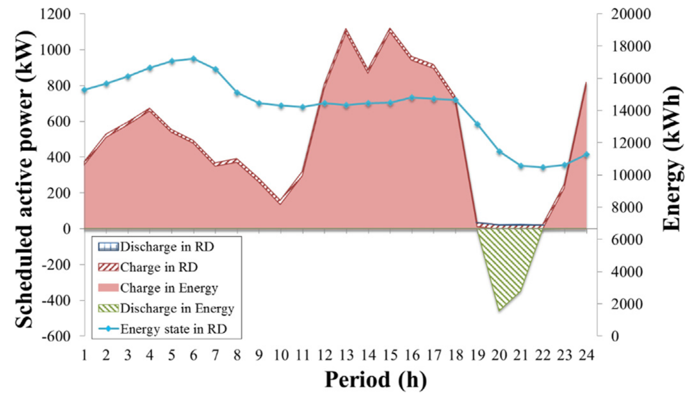

Fig. 12. Electric vehicles charge and discharge for the RD service. (For interpretation of the references to colour in this figure citation, the reader is referred to the web version of this article.)

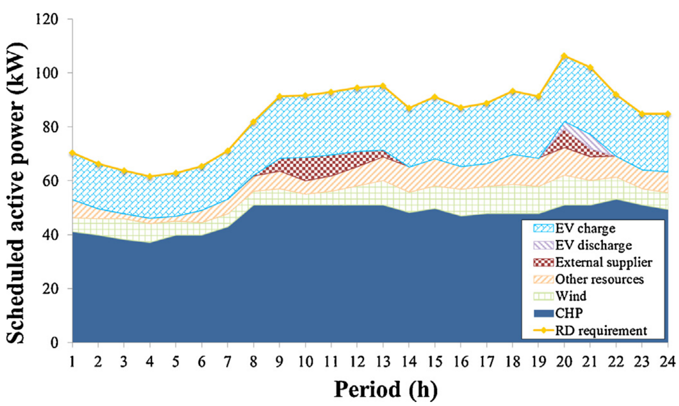

Fig. 10. Energy resource scheduling for the regulation down service.

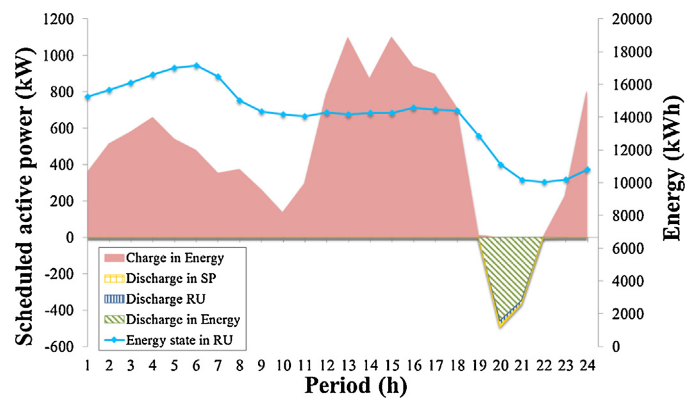

Fig. 13. Electric vehicle charge and discharge for the RU, SP and NS services.

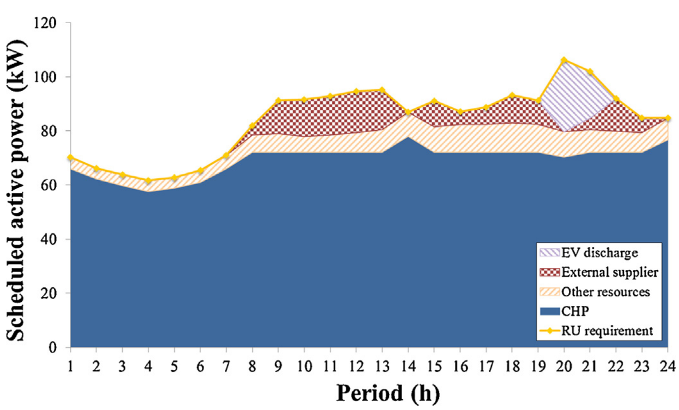

Fig. 11. Energy resource scheduling for the regulation up service.

be used in all periods, instead of using more expensive resources. EVs discharge is also used in the regulation down (by reducing the discharge level), in particular in peak periods, but with a smaller impact when compared with EVs charge in this service. Thus, it is expected that most of the EVs charge will be in the regulation down service, where both VPP and EV users can have technical and economic benefits. On the other hand, the EVs discharge is used in the RU service as it is shown in Fig. 11. In this service, the EVs are namely used in peak periods. In the spinning reserve service, EVs have a smaller impact, but they are also used in the peak periods. In the non-spinning reserve service, the EVs are not used and the ERS^{2}A algorithm dispatched other resources (DG and external suppliers) in this service. Thus, EVs discharge will be more common in the regulation up services than in the others, namely for solving the power imbalance during peak periods.

Fig. 12 presents the EVs charge and discharge scheduling for the RD service of the best ERS^{2}A solution. In this figure, the blue line represents the energy stored by the EVs batteries at the end of each period. In the regulation down, EVs charge is used in all periods, but they have a small impact when compared with the charge and discharge in the energy service. The EVs charge and discharge power for the RU, SP and NS services are shown in Fig. 13. In this case, the EVs' discharge is more used in the peak periods, and it is possible to see the use of EVs in regulation up and spinning reserve services for periods 20 and 21.

5. Conclusions

The energy resource scheduling simulated annealing algorithm is proposed to determine the optimal resource scheduling for the energy and ancillary services joint management, considering an intensive use of electric vehicles. The objective function of the optimal resource scheduling minimizes the operation cost of the available resources for the next day. The optimization problem considers the dispatch of energy, regulation down, regulation up, spinning reserve and non-spinning reserve. The main contribution of this paper lies on the modifications to adapt the ERS^{2}A algorithm to solve a day-ahead optimal resource scheduling for the energy and AS joint management with intensive EVs penetration. The main changes are in the initial solution and in the generation of a neighbour solution in order to deal with the four frequency control services. Another contribution is related to the application of the joint energy and AS scheduling to a VPP acting in a distribution network with a large DERs penetration, namely EVs.

The case study proves the effectiveness of using the ERS^{2}A algorithm to solve the joint management of energy and AS services. The proposed SA algorithm obtained an operation cost of 8706.06 m.u. that is very close to the optimal one obtained by the MINLP approach, presenting a small difference of 1.03%. In terms of simulation time, the proposed ERS^{2}A algorithm required a much lower execution time than the one achieved by the MINLP approach. The ERS^{2}A run in 70.70 s, while the MINLP took around 33.17 h to present the optimal solution. The ERS^{2}A algorithm presents encouraging results to be used by a VPP in a competitive environment, as it is characterized the smart grid environment.

Besides the main contribution of this paper, this work has allowed to reach a number of practical conclusions. The most important are that: (i) most of the EVs charge used in AS is applied to the regulation down in all periods; (ii) EVs discharge used in AS are more applied to the upward regulation (namely regulation up) in the peak periods; and (*iii*) ERS^{2}A methodology presented a good performance for simulation of large-scale management of distributed energy resources. This latter conclusion is relevant for a VPP that requires testing several scenarios with differences in the EVs data, such as trip distance and geographical location. The proposed ERS^{2}A algorithm can be used by the VPP to test different scenarios without spending too much time and without compromising the solution quality.

Acknowledgements

This work is supported by FEDER Funds through the "Programa Operacional Factores de Competitividade – COMPETE" programme and by National Funds through FCT "Fundação para a Ciência e a Tecnologia" under the projects FCOMP-01-0124-FEDER: UID/EEA/00760/2013, and SFRH/BD/81848/2011 (Tiago Sousa PhD), and by the SASGER-MeC, project no. NORTE-07-0162-FEDER-000101, co-funded by COMPETE under FEDER Programme. Tiago Soares is partly supported by the Denmark Technical University through a Ph.D. grant, as well as by the Danish Council for strategic research through the "5s – Future Electricity Markets" project (no. 12-132636/DSF). Hugo Morais is supported by the SOSPO project has received funding from the Danish Council for Strategic Research under grant agreement no. 11-116794. Rui Castro is supported by national funds through FCT "Fundação para a Ciência e a Tecnologia" with reference UID/CEC/50021/2013.

References

[1] J. Notenboom, P. Boot, R. Koelemeijer, J. Ros, Climate and Energy Roadmaps Towards 2050 in North-Western Europe, PBL Netherlands Environmental Assessment Agency, 2012.
[2] European Commission, Energy 2020 a strategy for competitive, sustainable and secure energy, in: COM(2010) 639 Final, 2010.
[3] G. Yang, T. Sun, J. Wang, X. Li, Modeling the nexus between carbon dioxide emissions and economic growth, Energy Policy 86 (2015) 104–117.
[4] D. Richardson, Electric vehicles and the electric grid: a review of modeling approaches, impacts, and renewable energy integration, Renew. Sustain. Energy Rev. 19 (2013) 247–254.
[5] O. Ellabban, H. Abu-Rub, F. Blaabjerg, Renewable energy resources: current status, future prospects and their enabling technology, Renew. Sustain. Energy Rev. 39 (2014) 748–764.
[6] R. Garcia-Valle, J. Lopes, Electric Vehicle Integration into Modern Power Networks, Springer, 2012.
[7] S. Ruiz-Romero, A. Colmenar-Santos, F. Mur-Pérez, Á. López-Rey, Integration of distributed generation in the power distribution network: the need for smart grid control systems, communication and equipment for a smart city — use cases, Renew. Sustain. Energy Rev. 38 (2014) 223–234.
[8] C. Gouveia, D. Rua, F.J. Soares, C. Moreira, P.G. Matos, J.A.P. Lopes, Development and implementation of Portuguese smart distribution system, Electr. Power Syst. Res. 120 (2015) 150–162.
[9] M. Fadaeenejad, A. Saberian, M. Fadaee, M. Radzi, H. Hizam, M. AbKadir, The present and future of smart power grid in developing countries, Renew. Sustain. Energy Rev. 29 (2014) 828–834.
[10] F. Mwasilu, J.J. Justo, E.-K. Kim, T.D. Do, J.-W. Jung, Electric vehicles and smart grid interaction: a review on vehicle to grid and renewable energy sources integration, Renew. Sustain. Energy Rev. 34 (2014) 501–516.
[11] P. González, J. Villar, C.A. Díaz, F.A. Campos, Joint energy and reserve markets: current implementations and modeling trends, Electr. Power Syst. Res. 109 (2014) 101–111.
[12] T. Zhang, H.B. Gooi, Hierarchical MPC-based energy management and frequency regulation participation of a virtual power plant, in: IEEE PES Innovative Smart Grid Technologies Conference Europe (ISGT-Europe), 2014, pp. 1–5.
[13] A.C. Rueda-Medina, A. Padilha-Feltrin, J.R.S. Mantovani, Active power reserve for frequency control provided by distributed generators in distribution networks, in: IEEE PES General Meeting|Conference & Exposition, 2014, pp. 1–5.
[14] R.J. Bessa, M.A. Matos, Global against divided optimization for the participation of an EV aggregator in the day-ahead electricity market. Part I. Theory, Electr. Power Syst. Res. 95 (2013) 309–318.
[15] M. Ghofrani, A. Arabali, M. Ghayekhloo, Optimal charging/discharging of grid-enabled electric vehicles for predictability enhancement of PV generation, Electr. Power Syst. Res. 117 (2014) 134–142.
[16] M. Yunfei, W. Jianzhong, J. Ekanayake, N. Jenkins, J. Hongjie, Primary frequency response from electric vehicles in the Great Britain Power System, IEEE Trans. Smart Grid 4 (2013) 1142–1150.
[17] W. Kempton, J. Tomic, Vehicle-to-grid power fundamentals: calculating capacity and net revenue, J. Power Sources 144 (2005) 268–279.
[18] D. Pudjianto, C. Ramsay, G. Strbac, Virtual power plant and system integration of distributed energy resources, IET Renew. Power Gen. 1 (2007) 10–16.
[19] K. Dietrich, J.M. Latorre, L. Olmos, A. Ramos, Modelling and assessing the impacts of self supply and market-revenue driven Virtual Power Plants, Electr. Power Syst. Res. 119 (2015) 462–470.
[20] M. Braun, P. Strauss, A review on aggregation approaches of controllable distributed energy units in electrical power systems, Int. J. Distrib. Energy Resour. Technol. Sci. Publ. 4 (2008) 297–319.
[21] H. Morais, T. Pinto, Z. Vale, I. Praca, Multilevel negotiation in smart grids for VPP management of distributed resources, IEEE Intell. Syst. 27 (2012) 8–16.
[22] S. Boyd, L. Vandenberghe, Convex Optimization, Cambridge University Press, 2004.
[23] T. Sousa, Z. Vale, J.P. Carvalho, T. Pinto, H. Morais, A hybrid simulated annealing approach to handle energy resource management considering an intensive use of electric vehicles, Energy 67 (2014) 81–96.
[24] G. Venayagamoorthy, Dynamic, stochastic, computational, and scalable technologies for smart grids, IEEE Comput. Intell. Mag. 6 (2011) 22–35.
[25] I. Boussaïd, J. Lepagnot, P. Siarry, A survey on optimization metaheuristics, Inform. Sci. 237 (2013) 82–117.
[26] S. Mahdavi, M.E. Shiri, S. Rahnamayan, Metaheuristics in large-scale global continues optimization: a survey, Inform. Sci. 295 (2015) 407–428.
[27] Z. Yang, K. Li, A. Foley, Computational scheduling methods for integrating plug-in electric vehicles with power systems: a review, Renew. Sustain. Energy Rev. 51 (2015) 396–416.
[28] D. Jost, M. Speckmann, F. Sandau, R. Schwinn, A new method for day-ahead sizing of control reserve in Germany under a 100% renewable energy sources scenario, Electr. Power Syst. Res. 119 (2015) 485–491.
[29] J. Pillai, B. Bak-Jensen, Integration of vehicle-to-grid in the Western Danish Power System, IEEE Trans. Sustain. Energy 2 (2011) 12–19.
[30] C. Battistelli, A.J. Conejo, Optimal management of the automatic generation control service in smart user grids including electric vehicles and distributed resources, Electr. Power Syst. Res. 111 (2014) 22–31.
[31] S. Han, S. Han, Development of short-term reliability criterion for frequency regulation under high penetration of wind power with vehicle-to-grid support, Electr. Power Syst. Res. 107 (2014) 258–267.
[32] E. Sortomme, M. El-Sharkawi, Optimal combined bidding of vehicle-to-grid ancillary services, IEEE Trans. Smart Grid 3 (2012) 70–79.
[33] E. Sortomme, M. El-Sharkawi, Optimal scheduling of vehicle-to-grid energy and ancillary services, IEEE Trans. Smart Grid 3 (2012) 351–359.
[34] N. Rotering, M. Ilic, Optimal charge control of plug-in hybrid electric vehicles in deregulated electricity markets, IEEE Trans. Power Syst. 26 (2011) 1021–1029.
[35] J. Zhong, L. He, C. Li, Y. Cao, J. Wang, B. Fang, L. Zeng, G. Xiao, Coordinated control for large-scale EV charging facilities and energy storage devices participating in frequency regulation, Appl. Energy 123 (2014) 253–262.
[36] R.J. Bessa, M.A. Matos, Optimization models for an EV aggregator selling secondary reserve in the electricity market, Electr. Power Syst. Res. 106 (2014) 36–50.
[37] T. Sousa, H. Morais, R. Castro, Z. Vale, A new heuristic providing an effective initial solution for a simulated annealing approach to energy resource scheduling in smart grids, in: 2014 IEEE Symposium on Computational Intelligence Applications in Smart Grid (CIASG), 2014, pp. 1–8.
[38] S. Peterson, J. Apt, J. Whitacre, Lithium-ion battery cell degradation resulting from realistic vehicle and vehicle-to-grid utilization, J. Power Sources 195 (2010) 2385–2392.
[39] J. Grainger, W. Stevenson, Power System Analysis, McGraw-Hill, 1994.
[40] California ISO, Business Practice Manual for Market Operations, 2015.
[41] D. Nock, V. Krishnan, J.D. McCalley, Dispatching intermittent wind resources for ancillary services via wind control and its impact on power system economics, Renew. Energy 71 (2014) 396–400.

[42] J. Ferreira, V. Monteiro, J. Afonso, Vehicle-to-anything application (V2Anything App) for electric vehicles, IEEE Trans. Ind. Inform. (2013) 1.
[43] J. Soares, B. Canizes, C. Lobo, Z. Vale, H. Morais, Electric vehicle scenario simulator tool for smart grid operators, Energies 5 (2012) 1881–1899.
[44] E. Dovgan, M. Javorski, T. Tušar, M. Gams, B. Filipič, Discovering driving strategies with a multiobjective optimization algorithm, Appl. Soft Comput. 16 (2014) 50–62.
[45] S. Kirkpatrick, C. Gelatt, M. Vecchi, Optimization by simulated annealing, Science 220 (1983) 671–680.
[46] P. Laarhoven, E. Aarts, Simulated Annealing: Theory and Applications, Reidel, Lancaster, Dordrecht, 1987.
[47] J. Trovão, P. Pereirinha, H. Jorge, C. Antunes, A multi-level energy management system for multi-source electric vehicles – an integrated rule-based metaheuristic approach, Appl. Energy 105 (2013) 304–318.
[48] Ž.N. Popović, V.D. Kerleta, D.S. Popović, Hybrid simulated annealing and mixed integer linear programming algorithm for optimal planning of radial distribution networks with distributed generation, Elect. Power Syst. Res. 108 (2014) 211–222.
[49] G. Zäpfel, R. Braune, M. Bögl, Metaheuristic Search Concepts: A Tutorial with Applications to Production and Logistics, Springer, Berlin, 2010.
[50] T. Sousa, J. Soares, Z. Vale, H. Morais, P. Faria, Simulated annealing metaheuristic to solve the optimal power flow, in: IEEE Power and Energy Society General Meeting, 2011, pp. 1–8.
[51] D. Thukaram, H.M.W. Banda, J. Jerome, A robust three phase power flow algorithm for radial distribution systems, Electr. Power Syst. Res. 50 (1999) 227–236.
[52] M. Silva, H. Morais, Z. Vale, An integrated approach for distributed energy resource short-term scheduling in smart grids considering realistic power system simulation, Energy Convers. Manage. 64 (2012) 273–288.
[53] S. Peterson, J. Whitacre, J. Apt, The economics of using plug-in hybrid electric vehicle battery packs for grid storage, J. Power Sources 195 (2010) 2377–2384.
[54] U.S. Department of Transportation, Summary of Travel Trends: 2009 National Household Travel Survey, 2011.